NOAA Technical Report ERL 395–APCL 42

Characteristics and Meteorological Impacts of Pollutants from the Kennecott Copper Smelter

F. Parungo
R. Pueschel
E. Ackerman
H. Proulx
D. Wellman

January 1978

U.S. DEPARTMENT OF COMMERCE
National Oceanic and Atmospheric Administration
Environmental Research Laboratories

NOAA Technical Report ERL 395–APCL 42

Characteristics and Meteorological Impacts of Pollutants from the Kennecott Copper Smelter

F. Parungo
R. Pueschel
E. Ackerman
H. Proulx
D. Wellman

January 1978

Boulder, Colorado

U.S. DEPARTMENT OF COMMERCE
Juanita Kreps, Secretary

National Oceanic and Atmospheric Administration
Richard A. Frank, Administrator

Environmental Research Laboratories
Wilmot Hess, Director

NOTICE

The Environmental Research Laboratories do not approve, recommend, or endorse any proprietary product or proprietary material mentioned in this publication. No reference shall be made to the Environmental Research Laboratories or to this publication furnished by the Environmental Research Laboratories in any advertising or sales promotion which would indicate or imply that the Environmental Research Laboratories approve, recommend, or endorse any proprietary product or proprietary material mentioned herein, or which has as its purpose an intent to cause directly or indirectly the advertised product to be used or purchased because of this Environmental Research Laboratories publication.

CONTENTS

CHARACTERISTICS AND METEOROLOGICAL IMPACT OF POLLUTANTS FROM THE KENNECOTT COPPER SMELTER

F. Parungo, R. Pueschel, E. Ackerman, H. Proulx, D. Wellman

Abstract. To study the meteorological impact of the pollutants released by the Kennecott Copper smelter, Salt Lake City, Utah, we collected airborne aerosol samples on Nuclepore filters in the plume at different distances from the stacks. Electron microscopes were used to analyze the morphology, concentration, and size distribution of the aerosols. An X-ray energy spectrometer was used to determine the elemental composition of the individual particles. Chemical and physical properties were related to cloud condensation and ice nucleation activities, which were measured with thermal diffusion chambers. We found that all the particles contained sulfur and were enveloped in a sulfuric acid liquid layer. The diameters of 95% of the particles were smaller than one micrometer. Most of the larger particles ($d > 0.5$ μm) consisted of Si, Fe, Cu, Ca and/or Mg. Most of the smaller particles ($d < 0.5$ μm) consisted of Pb, As, Se, Sn, etc. Because of their hygroscopic acidic surface, the aerosols are active cloud condensation nuclei. The ice nucleation activity of the aerosol was found to increase with distance downwind. In conjunction with long atmospheric residence time due to the small size of the particles, long-range transport and effect on mesoscale cloud structures are possible.

1. INTRODUCTION

The scientific community and the public have been greatly concerned about inadvertent weather modification resulting from air pollution. Large concentrations of aerosols released from industry can increase condensation or ice nucleus budgets, modify cloud microphysics, and influence precipitation downwind from the sources. Nevertheless, research on air pollution as a cause of weather modification is still controversial and inconclusive. To understand the mechanism for inadvertent weather modification by anthropogenic aerosols, we investigated the Kennecott Copper Corp. smelter plume because it is rich in sulfates, heavy metals, and SO_2.

The Kennecott Copper smelter, located near Magna, Utah, by the south shore of the Great Salt Lake, has operated with practically the same basic facility since 1904 to extract copper from ore. The crude ore mined at the Bingham Canyon open-pit mine contains copper sulfide (>0.4% Cu), iron sulfide, molybdenum, lead, gold, silver, etc. The ore is concentrated by a flotation process prior to smelting. The concentrated ore (25% Cu) is first smelted in reverberatory furnaces to separate copper and iron sulfides from siliceous slag. The resulting copper matter (40% Cu) is transferred to converter furnaces where sulfide reacts with high-pressured air to form SO_2 and produces 98.5% copper. In both kinds of furnaces sulfur dioxide is the major exhaust gas. Sulfuric acid and particulates are also expelled from the furnaces and emitted into the atmosphere through the stacks (Tayler, 1975). In general, the winds blow from the northwest across the Great Salt Lake, carry the plume along the southern side of the Oquirrh mountain range, and disperse it into the valley of Salt Lake City.

To study the meteorological impact of the pollutants from the smelter, we studied the characteristics of the aerosols in the plume. We flew an instrumented aircraft (Cessna 206) in and around the plume to collect samples. The plume was located with a sulfur dioxide sensor. Particulates were collected on Nuclepore filters (0.1 μm pore) with an isokinetic sampler and on an electron-microscope copper screen with an impactor. We investigated the morphology, chemical composition, concentration, and size distribution of the aerosol. We also measured cloud condensation nucleation activity and ice nucleation activity so that we could interpret the effect of these anthropogenic aerosols on cloud formation and precipitation.

2. MORPHOLOGY OF THE PARTICLES

We used a Coates and Welter scanning electron microscope (SEM), resolution 100 Å, and an RCA transmission electron microscope (TEM), resolution 10 Å, to study the morphology of the particles. Plume aerosols isokinetically collected represent the true concentration and size distribution. The sample on Nuclepore filter was coated with carbon and inserted directly in the SEM specimen chamber for observation. Figure 1 shows images of the particles. The pore size (0.1 μm) can be used as the length-measurement standard. Samples collected near the stack contain individual spheric particles, and samples collected at a distance downwind contain individual spheres, crystals, or agglomerates. For comparison, we examined dust from the base of the stack and from a deserted electrostatic precipitator of the smelter. Figure 2 shows that both samples are agglomerates of spherical, crystalline, and irregular particles.

We also examined the samples with the TEM, which provides better resolution than the SEM. Because the TEM beam cannot penetrate the filter, Ackerman (née Frank) developed a method to replicate the samples on a silicon monoxide (SiO) film and dissolve the Nuclepore filter with chloroform (Frank et al., 1970). Figure 3 shows micrographs of four samples collected at different distances from the stack. The samples collected near the stack appear as droplets enclosed with particles; at 10 km downwind, the droplets seem to be growing and solidifying; at 15 km, many orthorhombic crystals appear; at 30 km, there are individual and agglomerated particles. Figure 4 shows aerosols collected above the plume (3 to 4 km MSL); the many agglomerates of spheres and crystals are a mixture of natural, city, and aged plume aerosols.

The impactor collected the plume aerosols anisokinetically. It tends to select large particles. However, the particles were deposited on Formvar film on an EM specimen screen which can be directly observed with a TEM. This eliminates the replication procedure and produces true images of particles. Figure 5a shows the TEM images of the aerosols, which appear as solids imbedded in liquid drops. Figures 5b and 5c show the TEM images of dust from the base of the stack and from the electrostatic precipitator.

When treated with water, approximately 50% (by weight) of the dust dissolved. The solution had a pH value between 1 and 2, which indicated that the particles are very acidic. In the high vacuum of the TEM, volatile material, such as H_2SO_4, evaporates and cannot be detected. We used a method, developed by Frank and Lodge (1967), to identify sulfuric acid morphologically with the TEM. When samples on Formvar film are shadowed with chromium, sulfuric acid will produce a unique appearance in which rings of small satellite particles surround a large nucleus particle. We observed many such formations in the plume sample as shown in Figure 6, left column (arrowed), indicating that many particles were enveloped with sulfuric acid. Because H_2SO_4 is very hygroscopic, the particles should be very active cloud condensation nuclei. When we treated the sample with ammonia (NH_3) prior to chromium shadowing, the sulfuric acid was neutralized to solid ammonium sulfate (Figure 6, right column) and no rings were observed. Comparing the micrographs of the NH_3-treated and NH_3-untreated samples, we observed that numerous very fine particles ($d<0.1\mu m$) appeared on the NH_3-treated samples. This indicated that a mist of sulfuric acid was present in the plume and was converted to $(NH_4)_2SO_4$. Such a mist can play an important role in the formation of haze.

Samples collected 10 or 20 km downwind showed fewer sulfuric acid droplets and more crystalline particles. It is possible that sulfuric acid droplets were neutralized with atmospheric ammonia to form solid particulates.

Near the stack

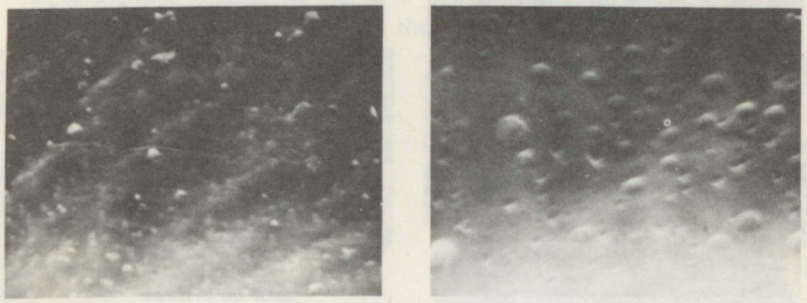

30 km downwind

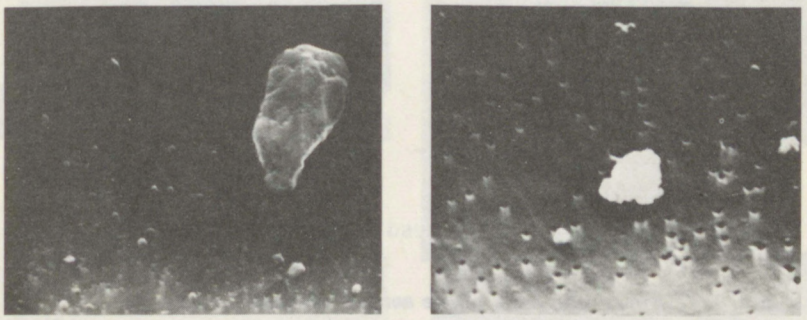

——1 μm (10,000 X) ——0.5 μm (20,000 X)

Figure 1. SEM micrographs of the plume aerosol on Nuclepore filters.

From the base of the stack

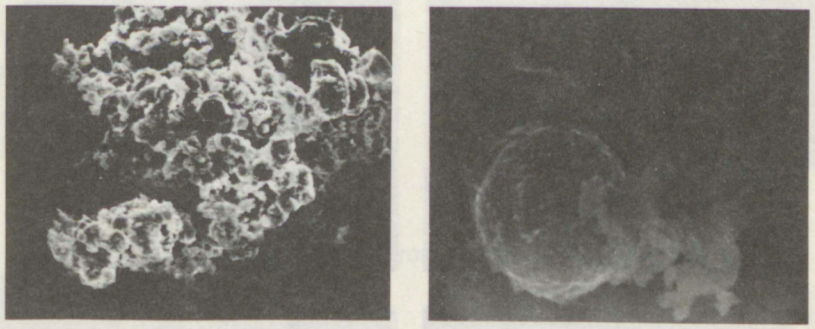

From the electrostatic precipitator.

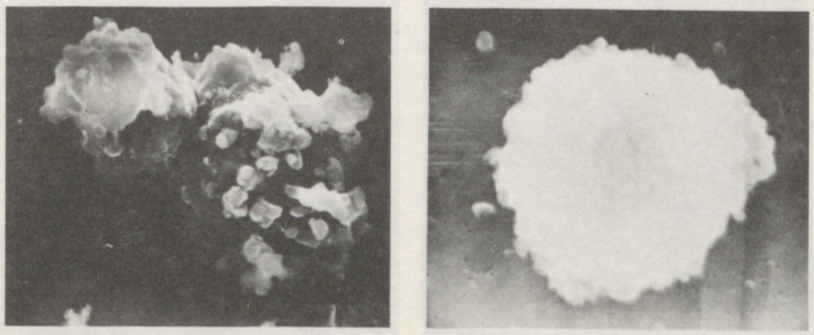

——1 μm (10, 000 X) ——0.5 μm (20, 000 X)

Figure 2. SEM micrographs of dust from the copper smelter.

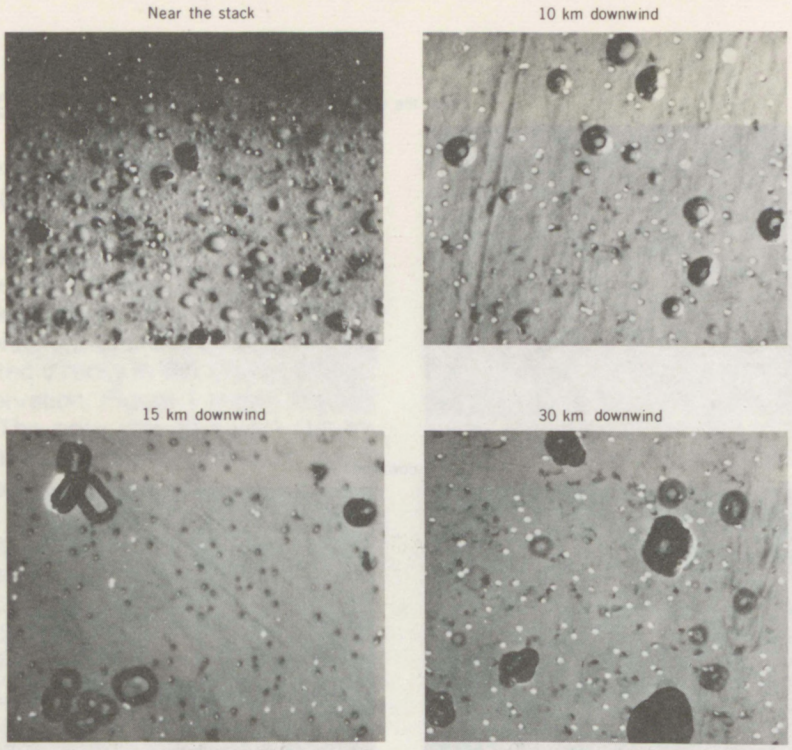

Figure 3. TEM micrographs of plume aerosol replicas.

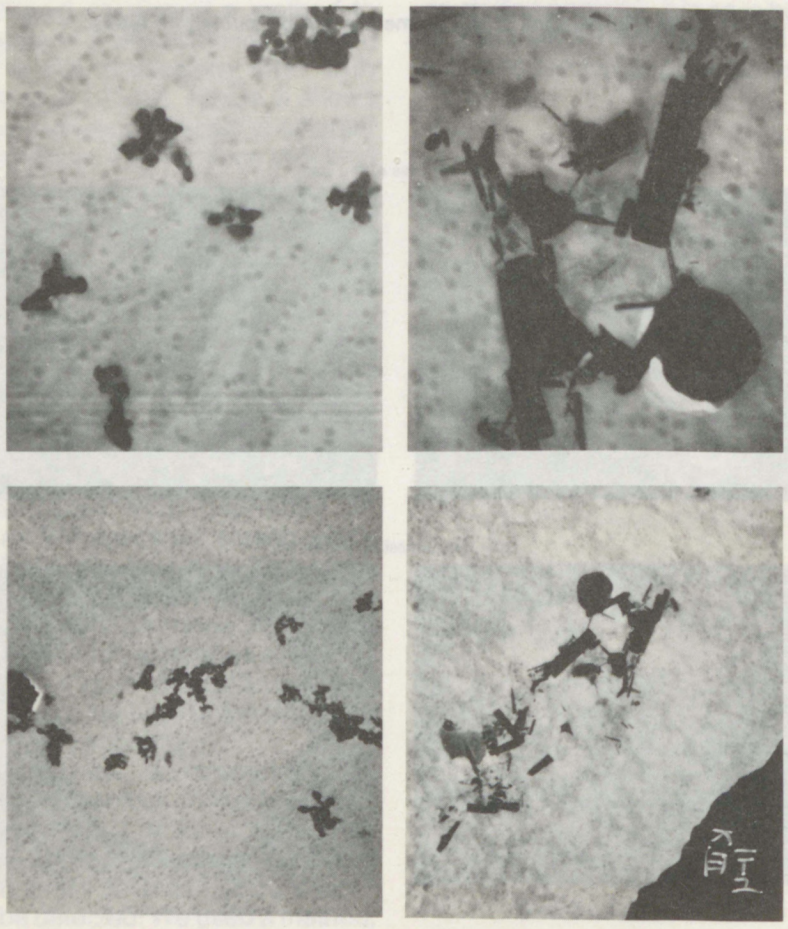

Figure 4. TEM micrographs of aerosols from above the plume.

a. From the plume.

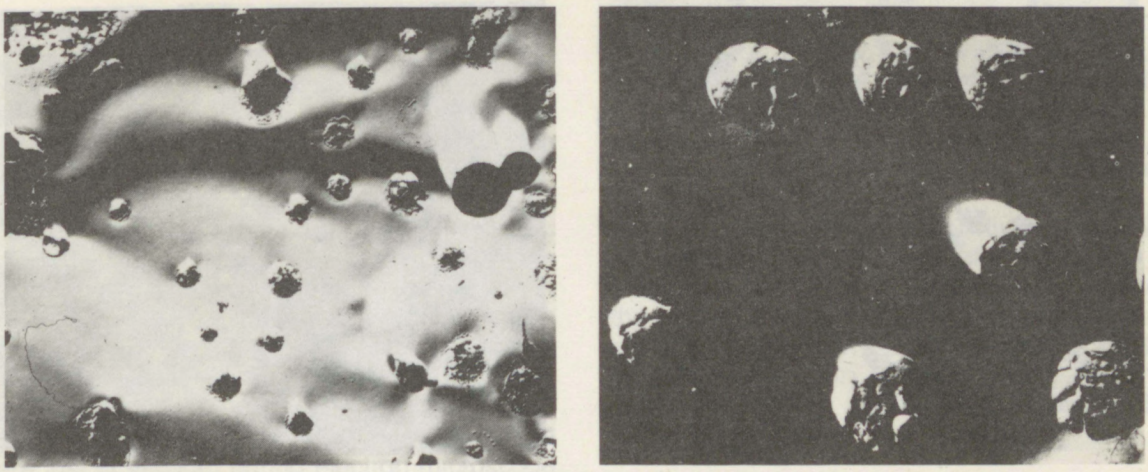

b. From the base of the stack.

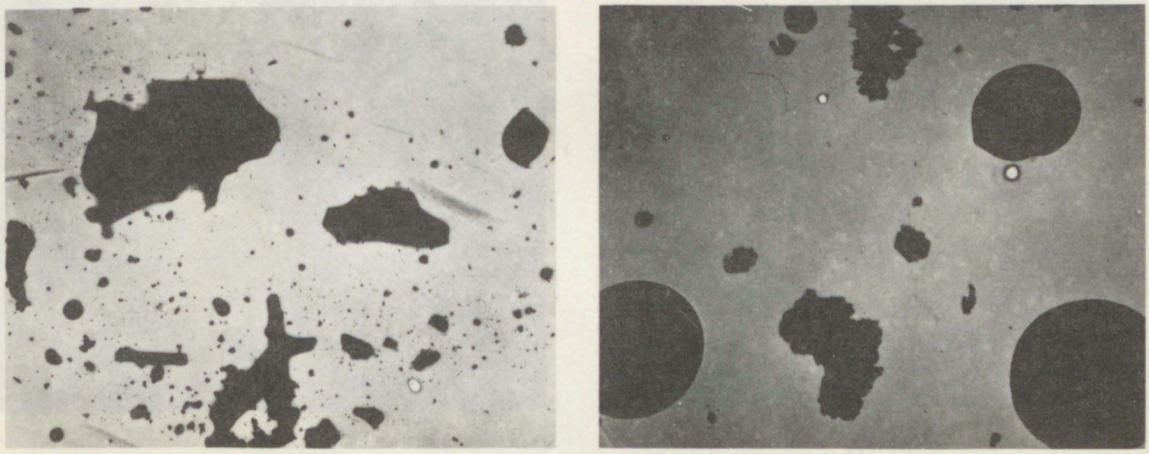

c. From the electrostatic precipitator.

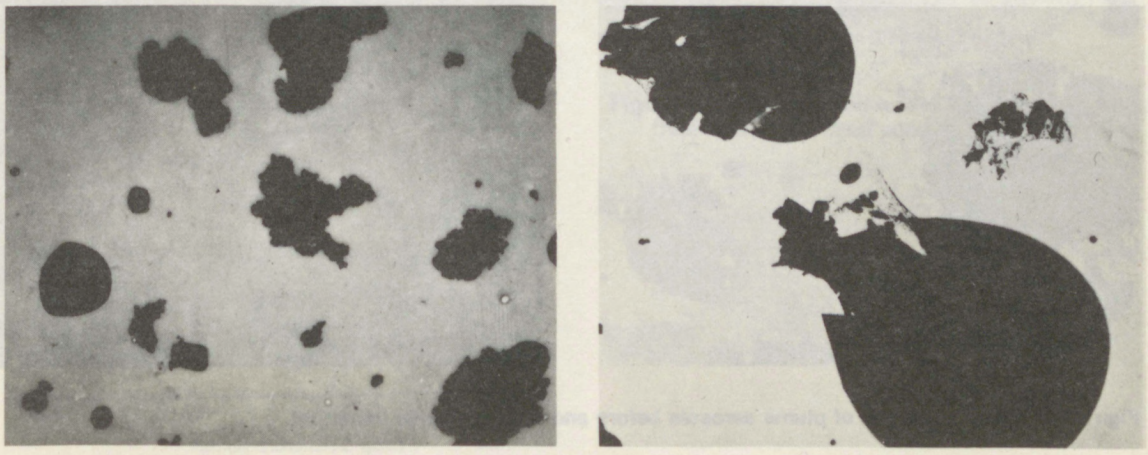

—1 μm (4,100 X)

—1 μm (12,300 X)

Figure 5. TEM micrographs of plume aerosols and dust.

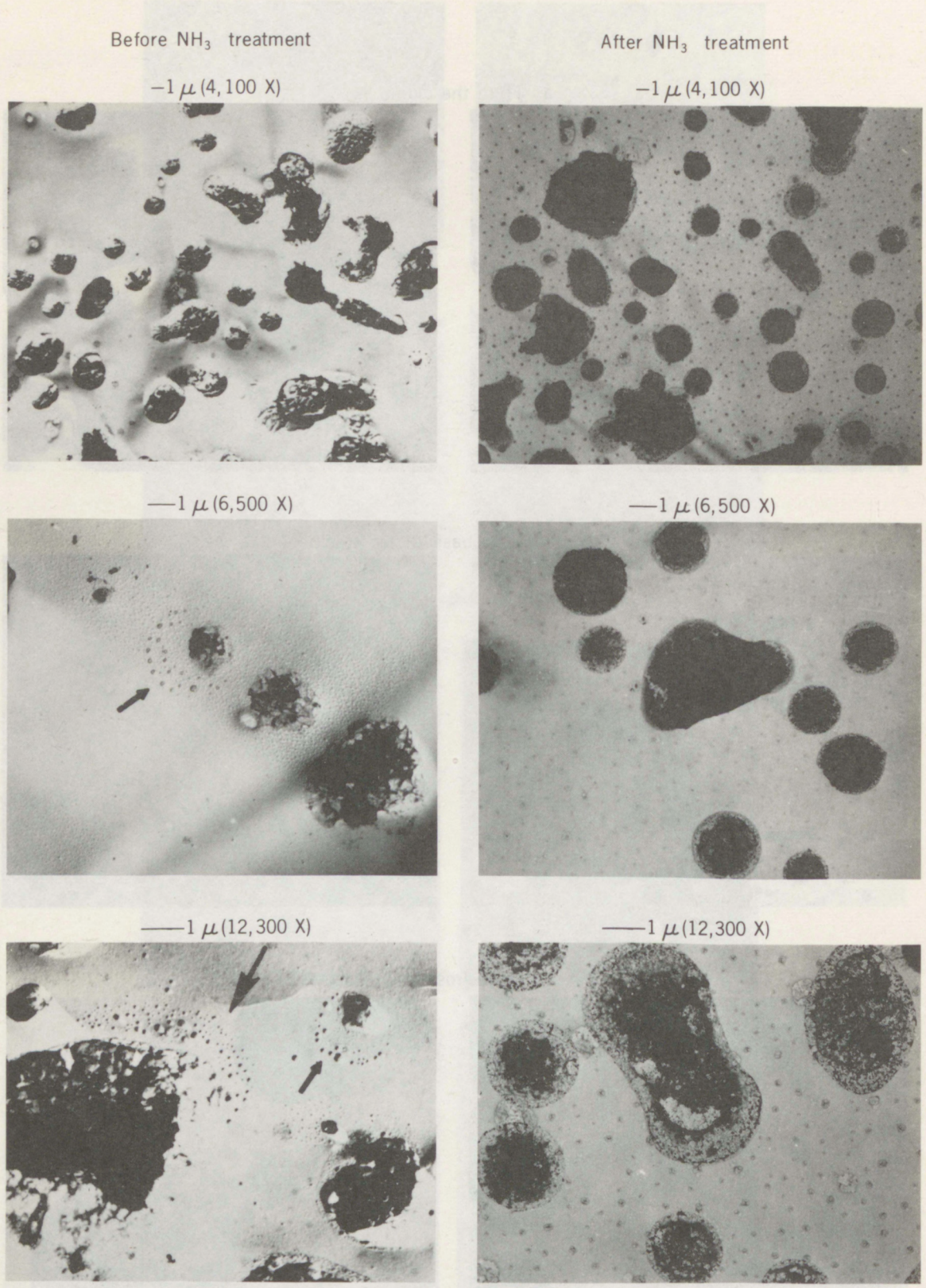

Figure 6. TEM micrographs of plume aerosols before and after ammonia treatment.

3. CONCENTRATION AND SIZE DISTRIBUTION OF THE PARTICLES

We used only samples that were collected isokinetically on Nuclepore filters for concentration and size distribution studies. Filter samples were replicated on SiO film and examined with the TEM. Figure 7 shows that near the stack the aerosol concentration was approximately 5×10^4 per cc with a mode of diameter at 0.1μm. Thirty km downwind from the source, the concentration decreased to 10^3 per cc and the diameter mode shifted to 0.2 μm. Aerosol concentration over Salt Lake City was approximately 5×10^3 per cc with major mode at 0.1 μm. However, particles coagulated to form larger particles. Thus a minor mode appeared at 1.0 μm.

Because sulfuric acid droplets evaporated and were lost in vacuum during electron microscope study, we exposed the sample filter to ammonia (NH_3) vapor to convert H_2SO_4 into $(NH_4)_2 SO_4$ and compared NH_3 treated samples with untreated samples. Figure 8 shows the differences between the four sets of samples. Near the stack, NH_3 treatment increased particle concentration three- to four-fold, indicating a high concentration of H_2SO_4 droplets. Farther downwind or over the city, concentration increased only a little, but the mode shifted to a larger size. Our interpretation is that most sulfuric acid droplets were neutralized by atmospheric ammonia or reacted with natural aerosols and the remaining free H_2SO_4 coated existing particles.

Figure 9 displays the cumulative size distribution, comparing particle sizes of the dust from the electrostatic precipitator, the dust from the base of the stack, and the sample taken in the plume. It indicates that the emission control device (electrostatic precipitator) tends to collect the larger particles; thus, the smaller particles escape into the atmosphere.

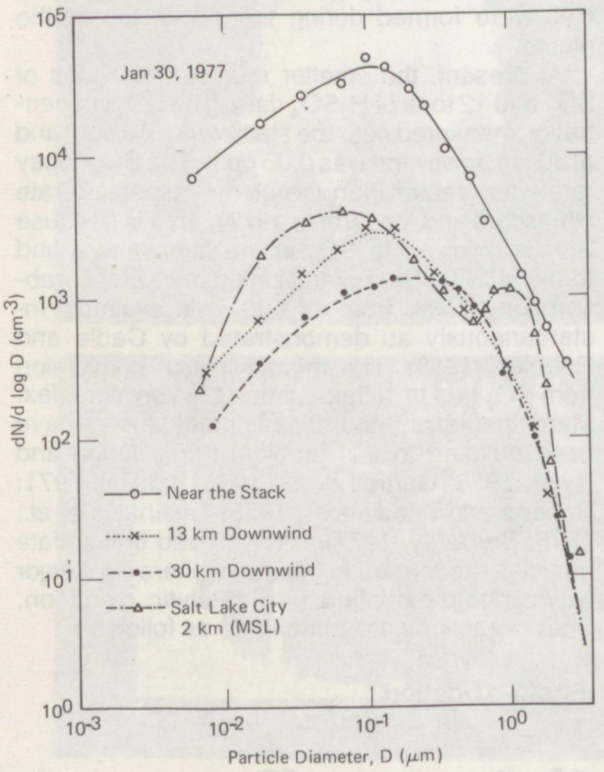

Figure 7. Concentration and size distribution of aerosols.

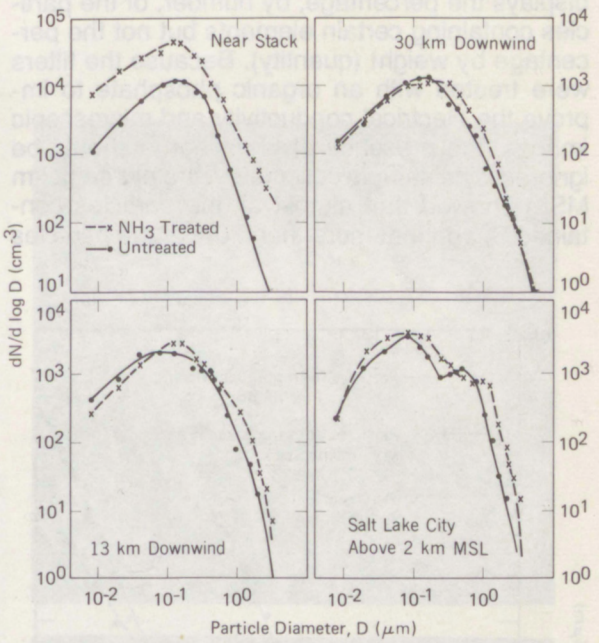

Figure 8. Concentration and size distribution of NH_3 treated and untreated aerosols.

4. CHEMICAL COMPOSITION OF THE AEROSOLS

We used an X-ray energy spectrometer (KEVEX) interfaced with an SEM to determine the elemental composition of individual particles. Particles with a diameter $> 0.05\ \mu m$, and all elements with an atomic number >10 can be analyzed simultaneously. Figures 10 and 11 show some examples of the images and the X-ray spectra of large and small particles. The horizontal scale of the spectra is the energy of the emitting X-rays in KeV, which identifies the elements; the vertical scale is the X-ray intensity, which reflects the quantity of each element present in the specimen. We made elemental identifications on the samples that were taken on 18 June 1976 five miles downwind of the smelter but at different altitudes. On each sample filter, we randomly selected 75 particles for analysis. The results are shown in Figure 12. It displays the percentage, by number, of the particles containing certain elements but not the percentage by weight (quantity). Because the filters were treated with an organic phosphate to improve the electrical conductivity and microscopic images, the presence of phosphorus should be ignored. The sample collected in the plume (2 km MSL) showed that almost all the particles contained S, and that more than 70% of the particles contained Na, Mg, Al, and Si. Toxic elements, such as As and Pb, were present in approximately 20% of the particles. In samples from higher altitudes (3 or 4 km MSL), where natural aerosols, city pollutants, and aged smelter exhaust have mixed, and where coagulation and sedimentation have occurred, 90% of the particles contained Si and 70% contained S. The presence of contaminants of other elements such as Pb and As was drastically reduced. Samples collected at ground level (1.4 km MSL) were similar to plume samples, except that they contained less S and more Fe.

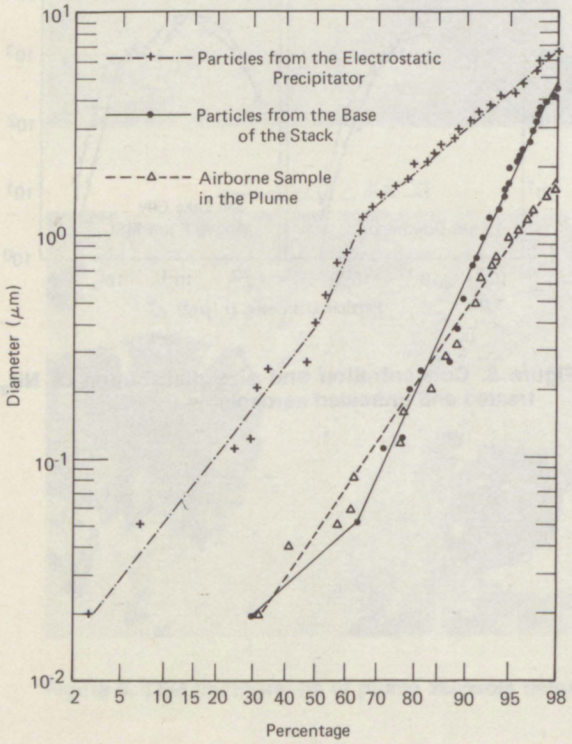

Figure 9. Cumulative size distribution of particles from different sources.

On 30 January 1977, samples were taken in the plume but at different downwind distances from the smelter. Unlike the previous samples, these samples did not have organic phosphate on the filters; therefore phosphorus could be detected. Figure 13 shows the results of the analysis. Ninety-eight percent of the aerosols collected near the stack contained S, 70% contained Pb, and 25% contained As. Farther downwind the plume aerosol settled, dispersed, and mixed with natural aerosols. The amount of Pb particles decreased to <10%, and of As particles to <2%. However, the amount of S particles decreased only to 75%. This demonstrated that significant S-containing particles were formed during the dispersion of the plume.

At present, the smelter releases 400 tons of SO_2 and 12 tons of H_2SO_4 daily. The SO_2 concentration measured near the stack was >10 ppm and at 30 km downwind was 0.05 ppm. The SO_2 decay rate was greater than the plume dispersing rate (Pueschel and Van Valin, 1977). This is because SO_2 is oxidized to SO_3 in the atmosphere and forms H_2SO_4. The neutralization of H_2SO_4 by absorption of NH_3 from air takes place almost instantaneously as demonstrated by Cadle and Robbins (1958). The mechanism of conversion from SO_2 gas to sulfate particles is very complex. Many theoretical and experimental studies have been devoted to this problem (e.g., Junge and Ryan, 1958; Gartrell et al., 1963; Bufalini, 1971; Roberts and Friedlander, 1975; Takahashi et al., 1975; Barbaray, 1977). It is believed that sulfate particles are formed in the atmosphere two major ways: photo-oxidation and catalytic oxidation. These reactions are formulated as follows:

Photo-oxidation

$$SO_2 + O \text{ (free radical)} \longrightarrow SO_3$$

$$SO_3 + H_2O \rightarrow H_2SO_4(v)$$

$$H_2SO_4(v) \xrightarrow[\text{nucleation}]{\text{homogeneous}}$$

$$H_2SO_4(v) + M \xrightarrow[\text{nucleation}]{\text{heterogeneous}} H_2SO_4 \cdot M(p)$$

The gas phase reaction between SO_2 and O_2 alone under tropospheric radiation ($\lambda > 2900$ Å) was very slow (oxidation rate = 0.04% h^{-1}, Kasahara and Takahashi, 1976). However, in the presence of substances that can provide oxygenated free radicals, photo-oxidation becomes an important removal process for SO_2. In the atmosphere the hydroxyl radical concentration was measured to be 10^6 molecules per ml; it has been claimed to be the major oxidant (Davis and Klauber, 1975). Furthermore, in the plume there are nitrogen oxides, ozone, and organic vapor which can also provide free radicals and enhance this photochemical reaction. Freiberg (1974) found that humidity is also a rate-determining factor. The photo-oxidation product SO_3 reacts almost simultaneously with ambient water vapor to form sulfuric acid vapor. This vapor can form sulfate aerosols by either homogeneous nucleation or heterogeneous nucleation. Goetz and Pueschel (1967) found that the presence of foreign particles is a dominant factor in the rate of aerosol formation.

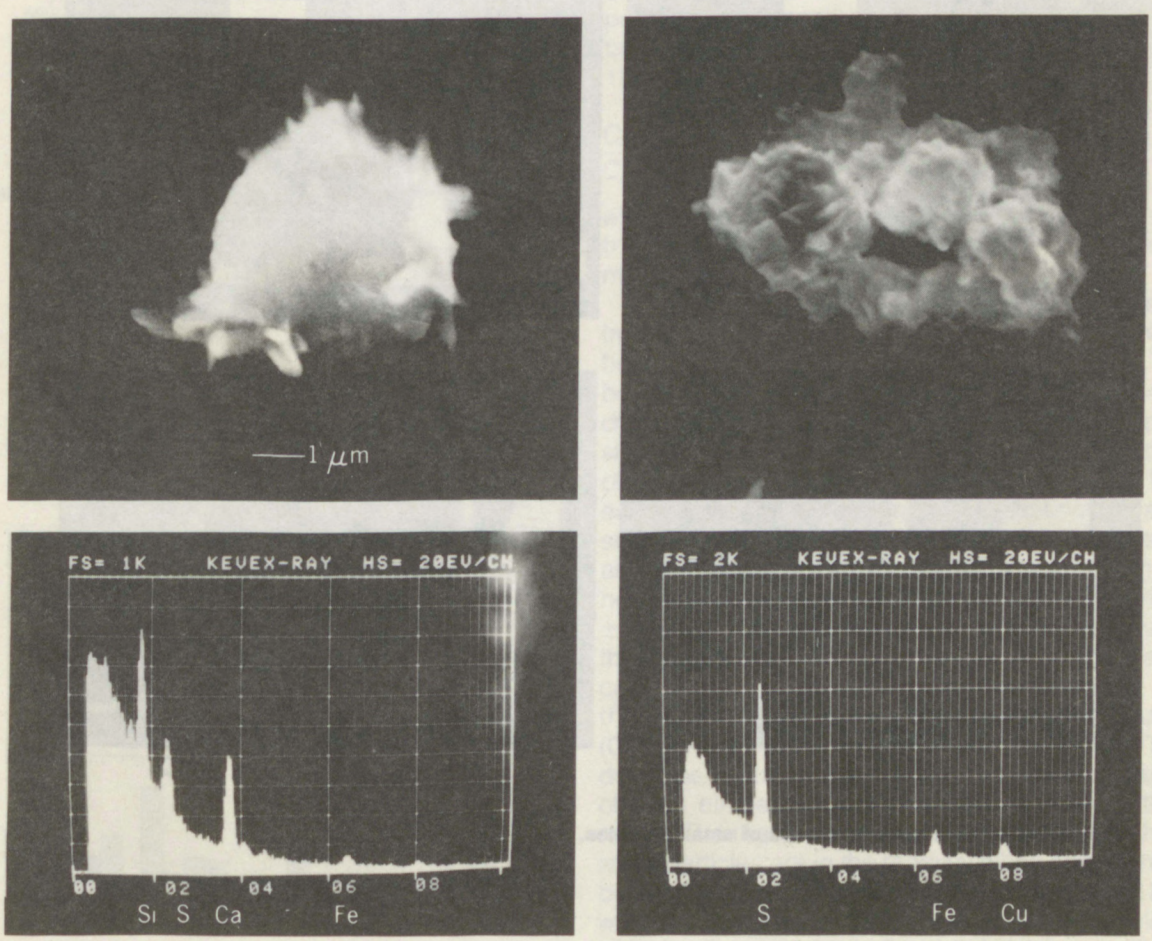

Figure 10. Images and X-ray spectra of two large particles.

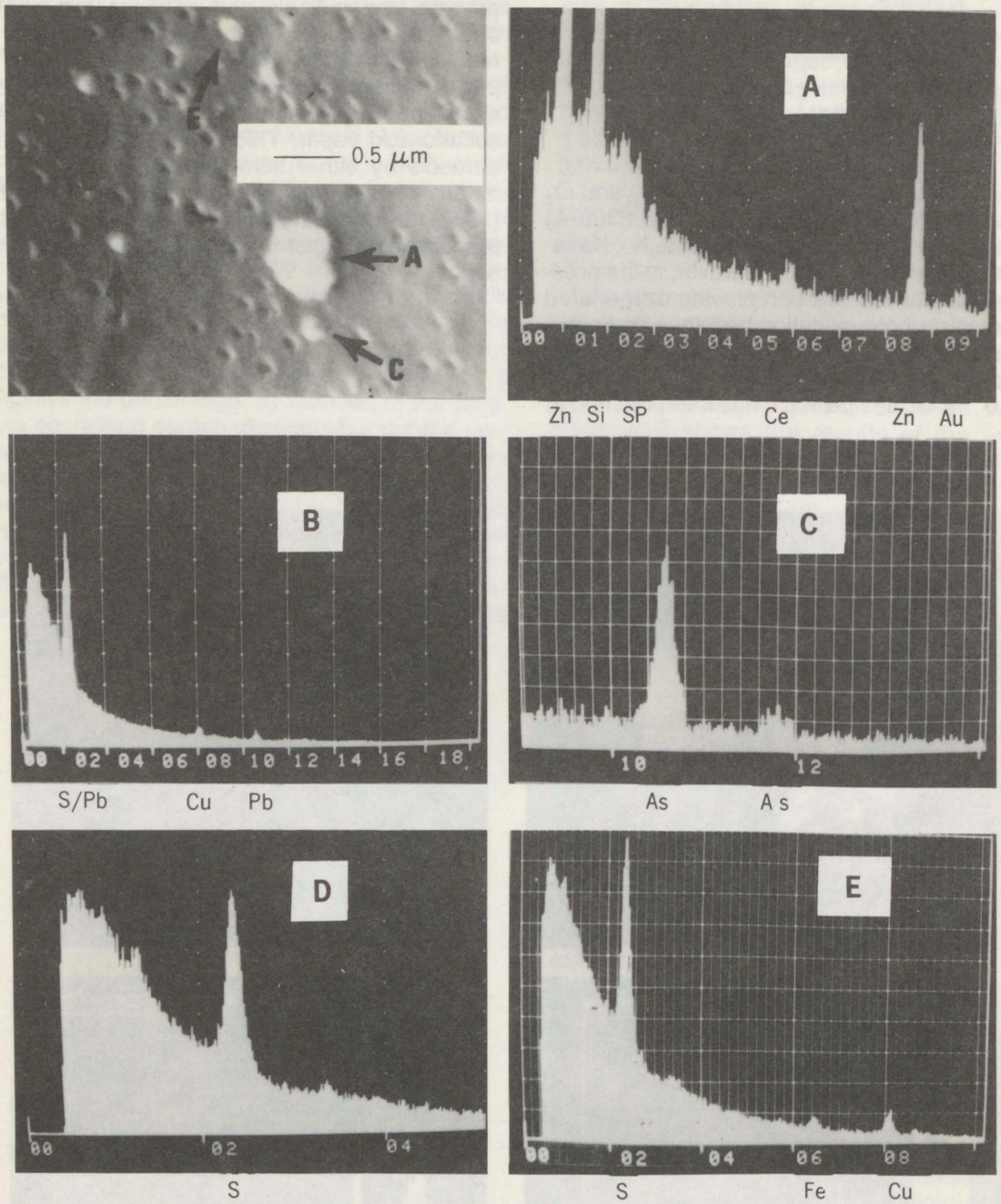

Figure 11. Images and X-ray spectra of small particles.

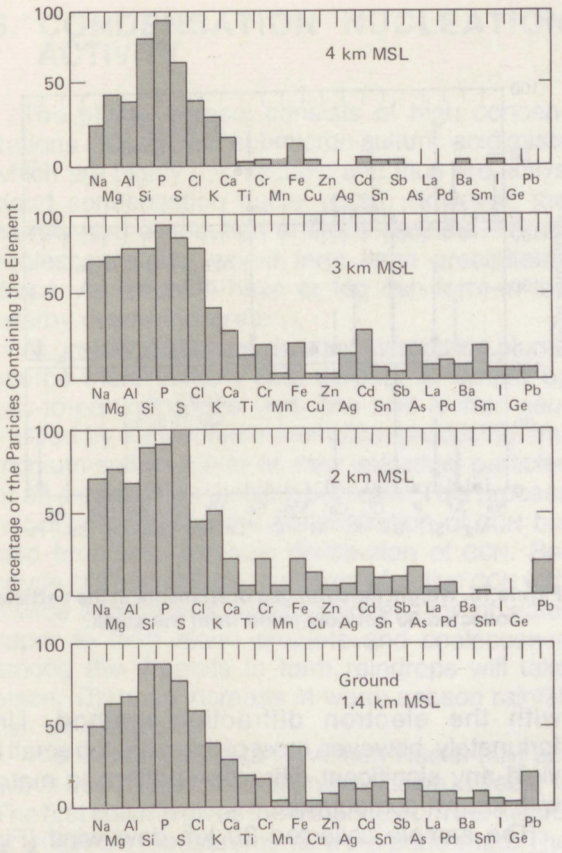

Figure 12. Elemental composition of aerosols collected at different altitudes.

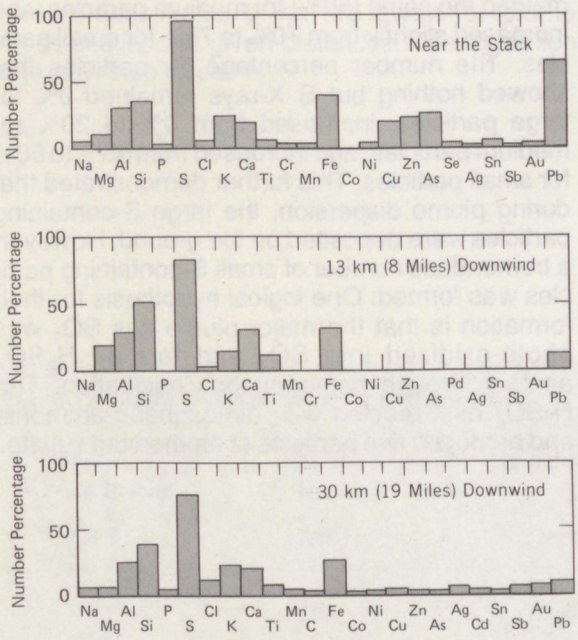

Figure 13. Elemental composition of aerosols collected at different downwind distances.

Catalytic oxidation

$$SO_2 + M \xrightarrow{O_2} SO_3 \cdot M \xrightarrow{H_2O} H_2SO_4 \cdot M$$

Smith et al. (1969) reported that sorption of SO_2 was 3% by Fe_3O_4 particles, 50% by Al_2O_3, and 100% by lead oxides. Urone et al. (1968) found that SO_2 in the presence of powdered oxides of Al, Ca, Cr, Fe, Pb, and V oxidized within minutes without ultraviolet irradiation. The plume aerosol contains numerous heavy metallic aerosols. When SO_2 vapor is adsorbed on these particles, it can be rapidly, catalytically oxidized to SO_3 and forms sulfate on the surface of the particles.

To study the relative importance of sulfate-forming mechanisms, it is necessary to know the sulfur concentration in each particle. Quantitative analysis by the SEM-XES system is still in its infancy. Because of fluctuations in instrumental conditions and the complex matrix of the particles, our analysis is only relative and semi-quantitative. We determined the relative concentrations of all the elements in individual particles from the ratios of their X-ray intensities. We calculated the weight percentage of each element in a particle on the basis of the following relationship (Hendricks, 1975):

$$\frac{Ci}{Cj} = \frac{Ii/Pi}{Ij/Pj}; \quad W\% = \frac{Ci}{\sum Ci} \times 100$$

where i and j are different elements, C is concentration, I is the X-ray intensity, and P is the elemental detection efficiency.

We kept the operational conditions on the spectrometer constant: accelerating voltage = 17 KV, beam current = 15 μA, magnification 75,000 ×, beam spot diameter = 90 Å, detector distance = 3 cm, and X-ray acquisition time = 60 sec. We measured the X-ray intensities of a series of standards of known concentrations. The relative P value for each element was determined. Because we assumed that the inter-element effect, matrix effect, and instrumental instability are negligible (which is not always true), the average error was found to be ±10%. The X-ray intensities of the elements and the weight percentages (Figs. 14 and 15) were calculated by computer. The particles are in three classes: large ($d > 2.0\ \mu m$), medium ($0.5\ \mu m < d < 2.0\ \mu m$), and small ($d \leq 0.5\ \mu m$). The dot in the figures is the average weight percentage of each element in that class, and the bar is the range. The reason for the size classification is that small particles are in the majority when considered by numbers, but in the minority when considered by weight; for example, the weight of 1000 particles with $d = 0.1\ \mu m$ equals the weight of one particle with $d = 1.0\ \mu m$. If we consider all the particles indiscriminately, the weight contribution of the small

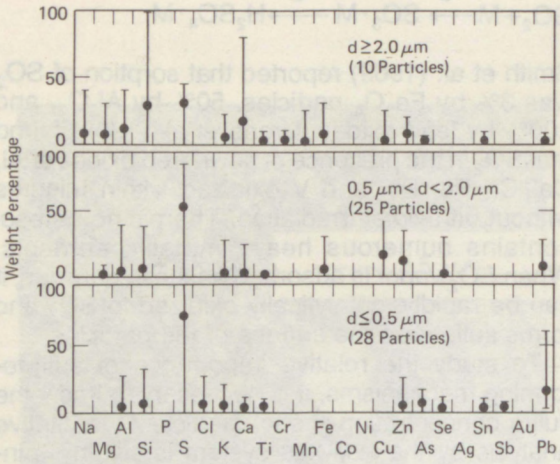

Figure 14. Weight percentages of elements in the particles collected near the stack.

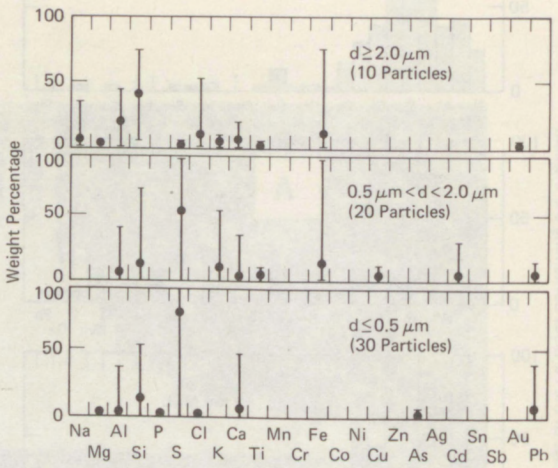

Figure 15. Weight percentages of elements in the particles collected 30 km downwind from the stack.

particles is negligible. However, these small particles are most important for cloud microphysics and effects on health. Therefore they should not be neglected.

In samples collected near the stack on 30 January 1977 (Fig. 14) large particles contained 0% to 45% of S by weight with an average of 30%; medium particles contained 0% to 90% of S with an average of 50%; and small particles contained 0% to 100% of S with an average of 70%. Particles that contained S and other elements are assumed to be sulfate salts; they are formed either by the catalytic oxidation between metallic aerosol and adsorbed SO_2 vapor, or by heterogeneous nucleation of sulfuric acid vapor on the plume aerosols. We found that large and medium particles are wholly metallic sulfates, and most of the small particles are also metallic sulfates. Thus, catalytic oxidation or heterogeneous nucleation is the dominant process for sulfate formation at the beginning. However, it is interesting to note that 15% of the small particles, indicated in the X-ray spectra, contained nothing but S. Pure S particles cannot survive the smelting process which must convert S to SO_2 or H_2SO_4 under 1500°C, with pressured air. Sulfuric acid (liquid) and SO_2 (vapor) cannot survive in the vacuum of the scanning electron microscope. Those particles showing only the sulfur X-ray are most likely ammonium sulfate, but could be organic sulfate. (The elements H, C, N, and O emit X-rays below the energy sensitivity of our instrument.) These small particles probably formed through homogeneous nucleation of H_2SO_4 vapor, and were instantaneously neutralized by ambient NH_3 to form ammonium sulfate particles. We attempted to identify such particles with the electron diffraction method. Unfortunately, however, most of them are too small to yield any significant diffraction pattern to match with known compounds.

The sample collected 30 km downwind (Fig. 15), shows that the average weight percentage of S is 75% in small particles, 50% in medium particles, and 2% in large particles. Compared with the sample collected near the stack, the S weight decreased from 30% to 2% for large particles, remained the same (50%) for medium particles, and increased slightly from 70% to 75% for small particles. The number percentage for particles that showed nothing but S X-rays remained 0% for large particles, increased from 0% to 20% for medium particles, and increased from 15% to 50% for small particles. This further demonstrated that during plume dispersion, the large S-containing particles were deposited on the ground. However, a tremendous number of small S-containing particles was formed. One logical hypothesis for their formation is that the major plume gas SO_2 was photo-oxidized into SO_3 and formed H_2SO_4 aerosol through homogeneous nucleation. The H_2SO_4 mist reacted with atmospheric ammonia and produced fine particles of ammonium sulfate.

5. CONDENSATION NUCLEATION ACTIVITY

The plume aerosol consists of high concentrations (10^4 cm^{-3}) of submicron sulfuric acid mists which are highly hygroscopic and thus are active cloud condensation nuclei (CCN). However, the narrow size distribution of these droplets inhibits coalescence that would form large precipitable drops. As a result, haze or fog can form in the nearby downwind area.

At greater distances downwind from the plume source more sulfuric acid aerosol is formed by gas-to-particle conversion. The acid is then neutralized by atmospheric ammonia, producing ammonium sulfate either as new individual particles or as a coating on existing particles. This process not only increases the concentration of CCN but also broadens the size distribution of CCN. Because of these greater numbers of active CCN with a wide spectrum of sizes, condensation of water vapor to form cloud droplets and coalescence among the droplets to form raindrops will take place. Thus, an increase in warm season rainfall can be expected.

The in-situ field data on Aitken Nuclei (AN) active at 200% supersaturation are shown in Table 1. The first column gives the distance from the stacks at which the measurements were performed. The second column gives quantities of AN measured with an Environment-One counter which was backed up by and calibrated with a Gardner counter. These concentrations are the net increase of aerosols within the plume. Horizontal and vertical fluxes of AN are given for plume cross-sections at given distances. The formation rate of Aitken nuclei is

$$\frac{\Delta AN}{\Delta t} = F_{L_2} - F_{L_1} + F_G$$

where F_{L_1} and F_{L_2} are the horizontal flux through the plume cross sections at distance L_1 and L_2, respectively, and F_G is the vertical flux to the ground. The nucleus flux calculations used a simple plume model (Turner, 1970) for atmospheric stability based on measured wind speeds and temperature lapse rates. The increase with distance of the rate of formation of Aitken nuclei appears puzzling at first and warrants further investigation. However, if viewed in the light of existing models for gas-to-particle conversion processes as mechanisms of aerosol formation, this phenomenon appears reasonable. The concentrations of oxidants such as O_3 and OH, and/or ammonia as a buffer, which all affect the rate of conversion of SO_2 to $SO_4^=$, are increasing because of the plume mixing with the environment as it travels to greater distances.

Because of some difficulties with the thermal diffusion cloud chamber, the in-situ field data on cloud condensation nuclei active at 1% supersaturation were not measured. Laboratory results indicate that in the Kennecott smelter dust about 50% of the Aitken nuclei are active as cloud condensation nuclei. This is to be expected because of the water solubility of sulfur particles which dominate in this aerosol.

Table 1. Aitken Nucleus Activity in the Plume*

Distance From Stacks L (km)	Aitken Nuclei (cm^{-3})	Horizontal Flux F_L (sec^{-1})	Vertical Flux F_G (sec^{-1})	ΔAN / Δt (sec^{-1})
−2	300			
3.2	166×10^3	1.1×10^{16}	7.6×10^{12}	1.1×10^{16}
12.8	8.5×10^3	2.4×10^{16}	2.1×10^{12}	1.3×10^{16}
30.4	17×10^3	2.0×10^{17}	1.1×10^{13}	2.0×10^{17}

*Variation with distance L from the stacks of Aitken nuclei (active at 200% supersaturation) concentrations, fluxes, and rates of formation measured on 30 January 1977 in the Kennecott Copper smelter plume.

6. ICE NUCLEATION ACTIVITY

Many methods are used to measure ice nuclei (IN). Since our samples are collected on Nuclepore filters, we are limited to using a membrane IN counter which counts ice crystals grown on the filter in a sub-freezing thermal diffusion chamber (Langer and Rodgers, 1975). One disadvantage of this method is that when condensation nuclei (CN) co-exist with IN, the CN are stronger competitors for moisture than IN, thus interfering with ice crystal growth. We found that the plume aerosol contains many hygroscopic particles such as sulfuric acid, sulfate, and chloride. When we measured IN at water saturation, the IN count in the plume aerosol averaged a few particles per liter compared with less than one particle per liter in a natural aerosol. When we applied excess moisture (3% supersaturation), the IN count increased more than ten-fold. Since we could not measure the moisture adsorbed by CN or the humidity around IN for initiating crystal growth, the counts of IN on filters must be considered relative values. We placed the sample filters side by side in the IN counter to compare IN activity as shown in Figure 16. Particle concentration decreased as distance from the stack increased; however, IN activity increased as distance increased. Parungo et al. (1977) reported that gases adsorbed on particles in the plume of a coal-fired power plant can deactivate IN activity. Since the gas concentration is higher near the stack, more IN are poisoned. To test this hypothesis, we placed the filters in a vacuum (10^{-4} torr) for 4 hours to get rid of volatile materials and found that IN activity increased by approximately one order of magnitude for the samples near the stack, but increased very little for the sample taken 30 km downwind. This experiment demonstrated that the plume particles that adsorb gases in the stack are not active ice nuclei, but can be activated as IN farther downwind when the volatile material evaporates during dispersion.

Langer (private communication, National Center for Atmospheric Research) installed an NCAR acoustic ice nucleus counter in an aircraft and flew in the plume of the Kennecott smelter. He measured IN concentrations as high as 10^4 l^{-1}. We used the same IN counter to test the dust collected in the smelter's electrostatic precipitator and at the base of the stack. We measured the number of particles introduced into the IN chamber and the number of ice crystals formed. The ratio between the two measurements is the fraction of particles forming ice crystals, or the probability of one particle becoming an active IN. The results are shown in Table 2. The probability of the dust from the precipitator forming ice nuclei was 5.55×10^{-4} and 2.06×10^{-3} at temperatures $-16°C$ and $-20°C$ respectively. The probability for dust from the stack was approximately one order of magnitude lower, 3.66×10^{-5} and 4.75×10^{-4} at $-16°C$ and $-20°C$ respectively. The electrostatic precipitator of the

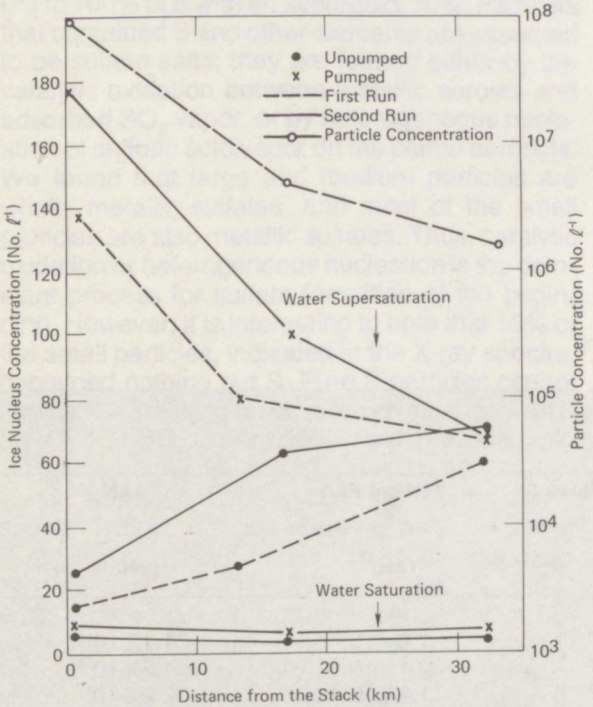

Figure 16. Ice nucleus concentration and particle concentration of plume aerosols.

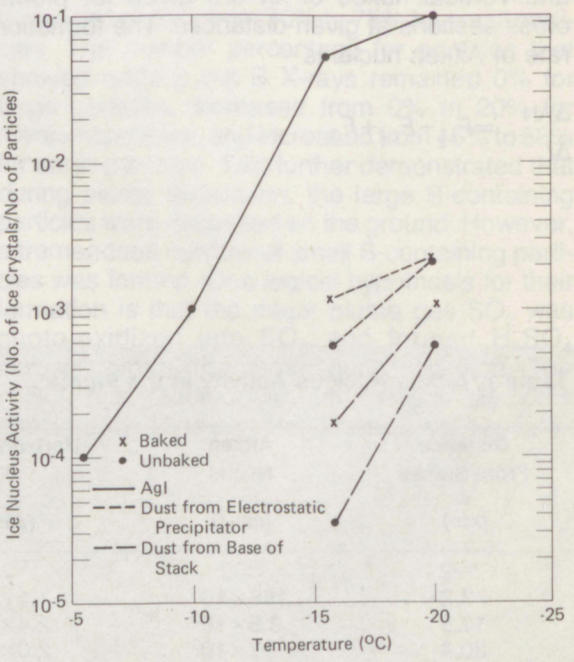

Figure 17. Ice nucleus activity of AgI and smelter dust.

smelter had been shut down for more than a year. The dust had been aged and some of the adsorbed gases may have escaped. This could be the reason for its higher activity.

To test whether or not the volatile material poisons ice nuclei, we baked both kinds of dust in an oven (200°C) for 5 hours and then tested their IN activity. The IN activity of baked stack dust increased approximately five-fold at −16°C and two-fold at −20°C; the IN activity of baked precipitator dust increased two-fold at −16°C and showed no change at −20°C. The test indicated that volatile materials indeed cause deactivation, and the poisoning effect is stronger at warmer temperatures (−16°C) than at colder temperatures (−20°C). To determine what the adsorbed gases are, we propose to use a gas-chromatograph interfaced with a mass spectrometer. However, this work has not been pursued because of lack of funding.

Figure 17 compares IN activities of the two kinds of smelter dust and silver iodide, which is one of the most active IN agents (Parungo et al., 1975). It shows that the IN activity of the dust is 2 to 3 orders of magnitude lower than AgI at −16°C but approximately 2 orders lower at −20°C. In cloud seeding operations, several kilograms of AgI aerosol are usually dispersed to increase precipitation. The smelter releases tons of dust per day. The total IN released from the smelter is far greater than the amount released by seeding operations. Therefore, the smelter's potential effect on ice nucleation in clouds and on snowfall downwind should not be neglected.

Table 2. Ice Nucleus Activity of Baked and Unbaked Dust.

	Baked Dust	Unbaked Dust	Ratio of Activity Fractions: Baked to Unbaked
Sample From Base of Stack			
No. of particles	287244	19430	
No. of ice crystals formed at −16°C	50	7	
No. of ice crystals formed at −20°C	292	91	
Fraction of particles forming ice crystals at −16°C	1.74×10^{-4}	3.66×10^{-5}	4.76
Fraction of particles forming ice crystals at −20°C	1.02×10^{-3}	4.75×10^{-4}	2.14
Sample From Electrostatic Precipitator			
No. of particles	248389	371403	
No. of ice crystals formed at −16°C	277	206	
No. of ice crystals formed at −20°C	514	765	
Fraction of particles forming ice crystals at −16°C	1.12×10^{-3}	5.55×10^{-4}	2.01
Fraction of particles forming ice crystals at −20°C	2.07×10^{-3}	2.06×10^{-3}	1.00

7. IMPLICATIONS TO LOCAL CLIMATE

The Kennecott Copper smelter has operated since 1904. Its average sulfur dioxide emission was as high as 1952 tons per day (T/D) in 1941. At present it has been reduced to 400 T/D by air pollution control. The emission of sulfuric acid is 12 T/D, and of solid particles 3 T/D (Dr. R. Heaney, Kennecott Copper Corp., private communication). Our laboratory study indicated that sulfuric acid mist and sulfate particles can adsorb moisture even at subsaturated humidity, and thus are active haze or fog-forming nuclei. Unfortunately, we do not have sufficient data on local air quality, visibility, and fog occurrence to make a statistical correlation between the plume emission and meteorological conditions. However, during our investigation in Salt Lake City, we often observed fog or mist in the morning and haze in the afternoon. A photograph, taken above a morning inversion layer (Fig. 18), depicts fog that covered the whole valley. Figure 19 shows the smelter plume dispersed toward the southeast and a thick layer of brown haze extending downwind from the smelter and along the mountain range. Apparently, if the smelter is not the sole source, it is probably a strong contributor to such anthropogenic meteorological conditions.

Among the best kept climatological data are precipitation records. Annual precipitation data of Salt Lake City (SLC) since 1892 are plotted in Figure 20. Before 1904, the average annual precipitation was 14.72 inches (34.6 cm) with a standard deviation $\sigma=2.56$. From 1905 to 1948 (when the downtown station was closed), the average was 16.11 inches (42.0 cm) and $\sigma=3.24$. The difference between the means for the two periods is 1.39 inches and is not significant. In 1928, a new weather station was added at SLC airport and it became the official SLC station in 1948, replacing the downtown station. The downtown station usually recorded precipitation one or two inches higher than the airport. If the airport data are included for calculation, the average precipitations for the two periods (before and after the smelter operation) are practically the same.

In section 5 we stated that concentration of condensation nuclei in the plume increased as the distance from the stack increased, because of gas-to-particle conversion. In section 6 we stated that ice nuclei can be reactivated by evaporating the adsorbed "poison gas" farther downwind. If the plume particles serve as condensation or ice nuclei to cause inadvertent weather modification, they should be more effective at distances farther from the smelter. As the plume travels, it mixes with SLC urban pollution and with emission from the U. S. Steel mill (30 miles south of SLC). The combined air mass further increases the ice nucleus budget. In addition, the mountains southeast of SLC provide an orographic lifting to the plume and the nuclei can interact with the clouds on the east or south side of the mountains. As a result, we would expect an increase of precipitation 50 to 100 miles downwind. However, the directions of winds vary from time to time, and a station may be in or out of the plume-affected area, depending on the meteorological condition at the time. Since analyzing all precipitation data of single stations is tedious work which may not produce a significant result, we reviewed instead the climatological data of the entire state of Utah. Ninety percent of Utah's weather stations are within 150 miles east and south of the smelter (Fig. 21). Annual precipitation data are shown in Figure 22, along with average daily sulfur emission of the Kennecott Copper smelter. The average annual precipitation for the period 1892–1904 was 10.81 inches (27.43 cm) with $\sigma=1.50$. From 1905 to 1946, the average precipitation was 14.21 inches (36 cm) and $\sigma=$ 2.68. An increase of 3.40 inches precipitation per year was obtained after the smelter began operation. In the early nineteen-forties, the average daily emission of sulfur was reported to be approximately 1000 tons; by the late forties, the emission was reduced to about 500 tons; and at present, it is 200 tons. The average annual precipitation after 1945 was 11.06 with $\sigma=$ 2.0, a reduction of 3.15 inches from the previous period. Unfortunately, we do not have data of sulfur emission from the smelter before the forties to correlate with the precipitation data. However, the apparent correlation of the increase and decrease of precipitation and of emission suggests to us that a thorough investigation of possible inadvertent weather modification would be worthwhile.

Climatological Data of Utah 1947 lists comparative annual precipitation for 45 years for two divisions, the Great Basin and the Colorado Basin (Fig. 21). Figure 23 shows precipitation for the two divisions. For the Great Basin, where 80% of the stations are within 50 miles east and south of SLC, the average precipitation through 1904 was 11.83 inches (30 cm) with $\sigma=$ 1.49, and after 1904 the average was 15.14 inches (38.46 cm) with $\sigma=$ 2.88, an increase of 3.31 inches. For the Colorado Basin, where most stations are from 50 to 150 miles southeast of SLC, the average precipitation through 1904 was 7.67 inches (19.48 cm) with $\sigma=$ 1.93 and after was 12.01 inches (30.51 cm) with $\sigma=$ 2.26, an increase of 4.32 inches per year. It appears the increase in precipitation is more significant farther downwind, in the Colorado Basin, than it is in the Great Basin area.

Figure 18. Photograph of the smelter plume and the fog covering the valley downwind.

Figure 19. Photograph of the smelter plume and haze.

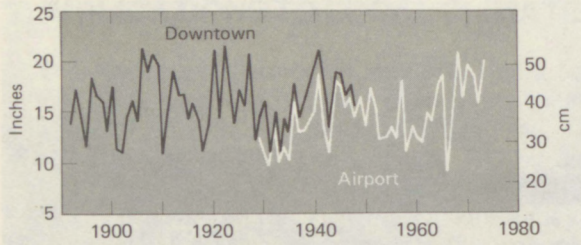

Figure 20. Total annual precipitation of Salt Lake City.

Climatological Data of Utah 1944 shows seasonal precipitation from 1891 through 1944 (Fig. 24). The difference between the periods before and after the beginning of smelter operation appears less significant in winter and spring but more significant for summer and autumn. Summer and autumn precipitation is essentially from convective clouds; winter and spring precipitation is generally from stratiform clouds. If the precipitation data reflect anthropogenic weather modification by smelter emission, the plume constituents seem to have a stronger seeding effect on convective clouds than on stratiform clouds. This is probably because stronger convection in the warmer seasons delivered the plume aerosols into the cloud-forming level where "rain-out" takes place.

Currently the Kennecott Copper smelter is being remodeled. Electrostatic precipitators are being installed to remove solid particles. Ninety percent of the SO_2 will be recovered and converted to H_2SO_4. A 1200 ft (366 m) stack is being built to lift the plume to a higher level. The new facility will be fully operational in 1978. Even if the new facility functions well and the emission meets Environmental Protection Agency standards, effects on local or regional meteorology may not be completely eliminated and new problems could arise. For example, most electrostatic precipitators usually collect the large particles only, and the small particles escape. If the large particles are not removed from the plume, the small particles can coagulate upon them and fall out close to the emission point. The large particles can also serve as heterogeneous nuclei for gas-to-particle conversion to reduce gas residential time. If only the large particles are removed from the plume, the small particles and gases can remain in the atmosphere for a long time and travel long distances, thus causing environmental impact at greater distances from the point of emission. In addition, the tall stacks will lift the pollution to the top of the boundary layer where cloud formation or interaction takes place, thereby increasing any meteorological impact. For the reasons mentioned, it would be interesting to monitor not only the aerosol chemistry farther downwind but also

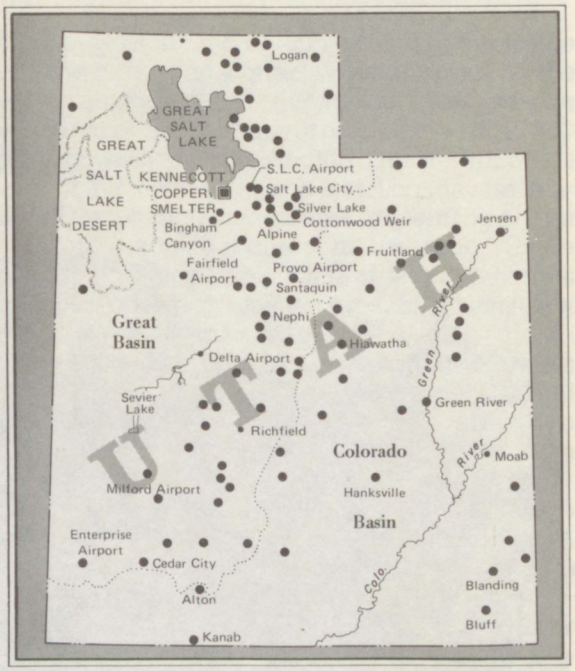

Figure 21. Locations of weather stations in Utah.

the meteorological conditions, such as air quality, visibility and precipitation in local and regional areas, and to compare them with old records. The information would be very useful to our understanding of inadvertent weather modification.

Because of lack of sufficient data on smelter emission and on local climate, we can only suggest that the emission from the Kennecott Copper smelter could inadvertently modify the regional weather. For a thorough investigation, we should measure in-situ ice nucleus and condensation nucleus concentrations of the plume at various locations. We should record the meteorological conditions, model the air mass journey, and project the affected area. Then we could compare precipitation data in the area with the projection. We are planning such experiments and hope to carry them out in the future.

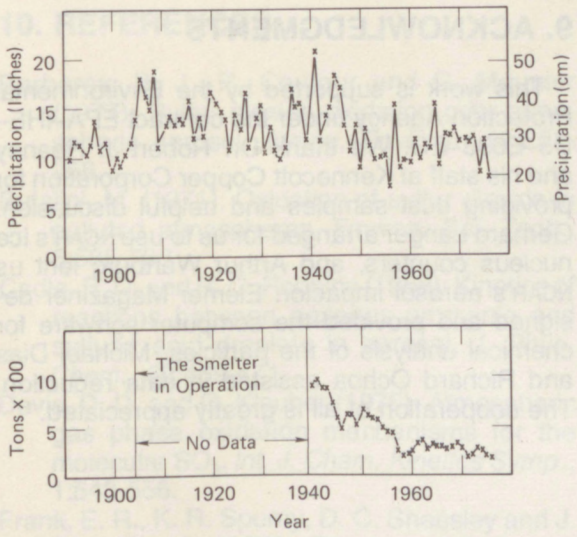

Figure 22. Annual precipitation of Utah and average daily sulfur emissions of the smelter.

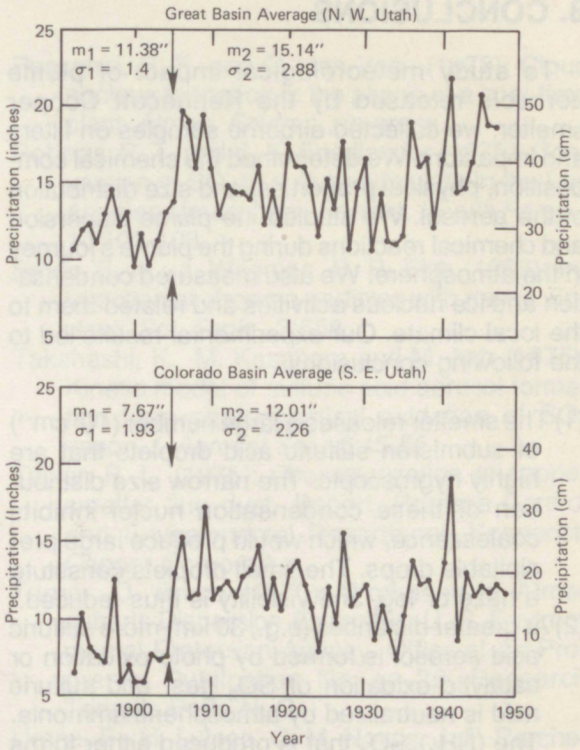

Figure 23. Annual precipitation of the two regions of Utah.

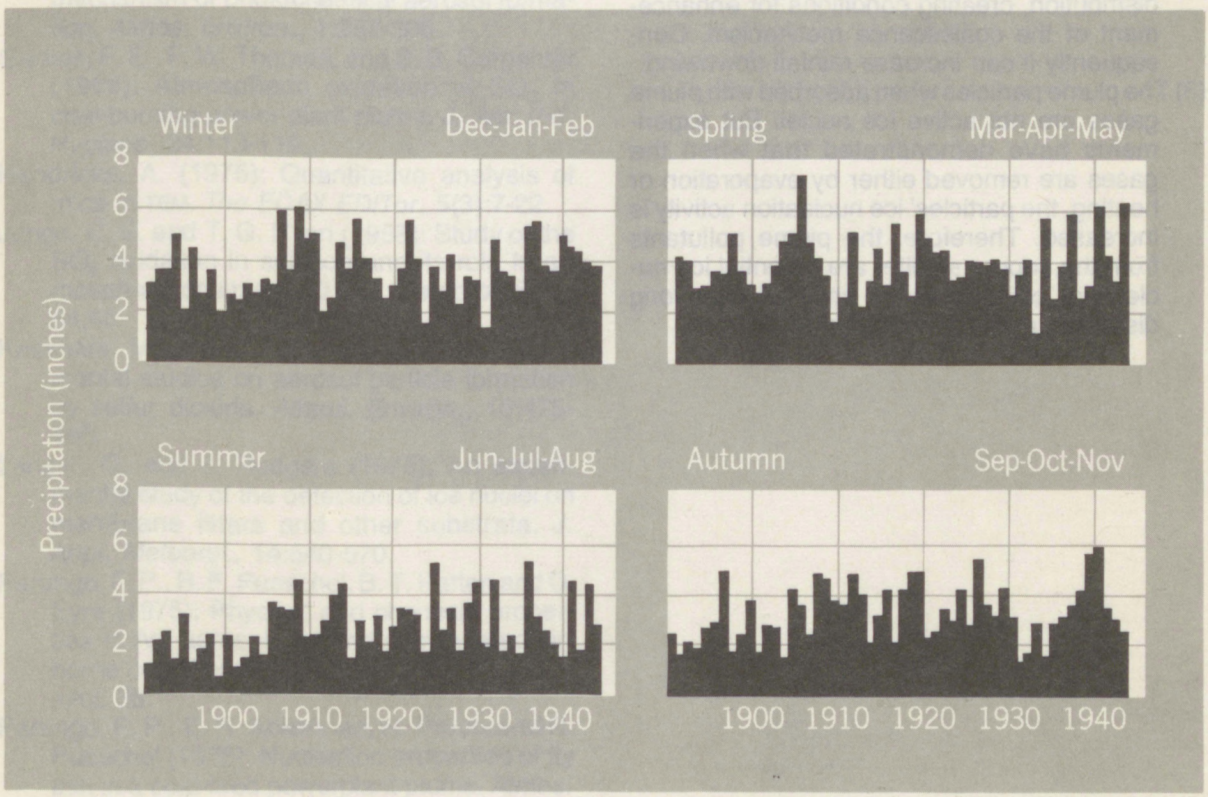

Figure 24. Seasonal precipitation of Utah.

8. CONCLUSIONS

To study meteorological impact of plume aerosols released by the Kennecott Copper smelter, we collected airborne samples on filters and impactors. We determined the chemical composition, physical properties, and size distribution of the aerosol. We studied the plume dispersion and chemical reactions during the plume's journey in the atmosphere. We also measured condensation and ice nucleus activities and related them to the local climate. Our experimental results led to the following conclusions:

(1) The smelter releases a large number (10^4 cm^{-3}) of submicron sulfuric acid droplets that are highly hygroscopic. The narrow size distribution of these condensation nuclei inhibits coalescence, which would produce large precipitable drops. The small droplets constitute a haze or fog, and visibility is thus reduced.

(2) At greater distances (e.g., 30 km) more sulfuric acid aerosol is formed by photo-oxidation or catalytic oxidation of SO_2 gas, and sulfuric acid is neutralized by atmospheric ammonia. The $(NH_4)_2SO_4$ that is produced either forms new particles or coats the existing particles. This increase in number and in size of condensation nuclei may broaden the droplet size distribution, creating conditions for enhancement of the coalescence mechanism. Consequently it can increase rainfall downwind.

(3) The plume particles when adsorbed with plume gases are not active ice nuclei. But experiments have demonstrated that when the gases are removed either by evaporation or heating, the particles' ice nucleation activity is increased. Therefore, the plume pollutants from the copper smelter are potential ice nuclei that could increase snowfall over long distances and extended periods of time.

9. ACKNOWLEDGMENTS

This work is supported by the Environmental Protection Agency under the contract EPA–IHE–D5–E693–EG. We thank Dr. Robert J. Heaney and his staff at Kennecott Copper Corporation for providing dust samples and helpful discussion. Gerhard Langer arranged for us to use NCAR's ice nucleus counters, and Arthur Wartburg lent us NCAR's aerosol impactor. Elemer Magaziner designed and provided the computer software for chemical analysis of the particles. Michael Dias and Richard Ochoa assisted in data reduction. The cooperation of all is greatly appreciated.

10. REFERENCES

Barbaray, B. J., P. Coutour and G. Mounier (1977): Sulfur dioxide oxidation over atmospheric aerosol. *Atmos. Environ.*, 11:351-356.

Bufalini, M. (1971): Oxidation of sulfur dioxide in polluted atmospheres. *Environ. Sci. Tech.*, 5:685-700.

Cadle, R. D. and R. C. Robbins (1958): Kinetics of reactions between gaseous ammonia and sulfuric acid droplets in aerosol. *J. Phys. Chem.*, 62:469-471.

Davis, D. D. and G. Klauber (1975): Atmospheric gas phase oxidation mechanisms for the molecular SO_2. *Int. J. Chem. Kinetics Symp.*, 1:543-556.

Frank, E. R., K. R. Spurny, D. C. Sheesley and J. P. Lodge, Jr. (1970): The use of Nuclepore filters in light and electron microscopy of aerosols. *J. Microsc.*, 9:735-740.

Frank, E. R. and J. P. Lodge, Jr. (1967): Morphologic identification of airborne particles with the electron microscope. *J. Microsc.*, 6:449-456.

Freiberg, J. (1974): Effects of humidity and temperature on SO_2 photo-oxidation. *Environ. Sci. and Tech.*, 8:731-734.

Goetz, A. and R. F. Pueschel (1967): Basic mechanism of photochemical aerosol formation. *Atmos. Environ.*, 1:287-306.

Gartrell, F. E., F. W. Thomas, and S. B. Carpenter (1963): Atmospheric oxidation of SO_2 in coal-burning power plant plume. *J. Am. Ind. Hygiene*, 24:113-119.

Hendricks, A. (1975): Quantitative analysis of mica in TEM. *The EDAX EDITor*, 5(3):7-22.

Junge, C. E. and T. G. Ryan (1958): Study of the SO_2 oxidation in solution and its role in atmospheric chemistry. *Q.J.R. Meteorol. Soc.*, 84:46.

Kasahara, M. and K. Takahashi (1976): Experimental studies on aerosol particle formation by sulfur dioxide. *Atmos. Environ.*, 10:475-486.

Langer, G. and J. Rodgers (1975): An experimental study of the detection of ice nuclei on membrane filters and other substrata. *J. Appl. Meteorol.*, 14:540-570.

Parungo, F. P., R. F. Pueschel, B. T. Patten and D. Eyre (1975): Physical and chemical properties of AgI aerosols formed at simulated airborne conditions, NOAA Tech. Rep. ERL 337–APCL 36.

Parungo, F. P., E. R. Ackerman, H. Proulx and R. Pueschel (1978): Nucleation properties of fly ash in a coal-fired powerplant plume. *Atmos. Environ.*, in press.

Pueschel, R. F. and C. Van Valin (1978): Cloud nucleus formation in the plume of a coal-fired plant. *Atmos. Environ.*, in press.

Roberts, P. T. and S. K. Friedlander (1975): Conversion of SO_2 to sulfur particulate in the Los Angeles atmosphere. *Environ. Health Persp.*, 10:103-108.

Smith, B. M., J. Wagman, B. R. Fish (1969): Interaction of airborne particles with gases. *Environ. Sci. Tech.*, 3:558.

Takahashi, K., M. Kasahara and M. Itoh (1975): Kinetic model of sulfuric acid aerosol formation from photochemical oxidation of SO_2 vapor. *J. Aerosol Sci.*, 6:45-55.

Tayler, P. L. (1975): Characterization of copper smelter flue dust. Report, Process Control and Environmental Department, Kennecott Copper Corporation.

Turner, D. Bruce (1970): Workbook of Atmospheric Dispersion Estimates, U. S. Environmental Protection Agency, Office of Air Programs, Publication No. AP–26, Research Triangle Park, N. C.

Urone, P., H. Lutsep, C. M. Noyes, J. F. Parcher (1968): Static studies of sulfur dixoide reactions in air. *Environ. Sci. Tech.*, 2:611-618.

☆ U.S. GOVERNMENT PRINTING OFFICE: 1978 — 777-067/1255 REGION NO. 8

Environmental Research LABORATORIES

The mission of the Environmental Research Laboratories (ERL) is to conduct an integrated program of fundamental research, related technology development, and services to improve understanding and prediction of the geophysical environment comprising the oceans and inland waters, the lower and upper atmosphere, the space environment, and the Earth. The following participate in the ERL missions:

MESA *Marine EcoSystems Analysis Program.* Plans, directs, and coordinates the regional projects of NOAA and other federal agencies to assess the effect of ocean dumping, municipal and industrial waste discharge, deep ocean mining, and similar activities on marine ecosystems.

OCSEA *Outer Continental Shelf Environmental Assessment Program Office.* Plans and directs research studies supporting the assessment of the primary environmental impact of energy development along the outer continental shelf of Alaska; coordinates related research activities of federal, state, and private institutions.

W/M *Weather Modification Program Office.* Plans and coordinates ERL weather modification projects for precipitation enhancement and severe storms mitigation.

NHEML *National Hurricane and Experimental Meteorology Laboratory.* Develops techniques for more effective understanding and forecasting of tropical weather. Research areas include: hurricanes and tropical cumulus systems; experimental methods for their beneficial modification.

RFC *Research Facilities Center.* Provides aircraft and related instrumentation for environmental research programs. Maintains liaison with user and provides required operations or measurement tools, logged data, and related information for airborne or selected surface research programs.

AOML *Atlantic Oceanographic and Meteorological Laboratories.* Studies the physical, chemical, and geological characteristics and processes of the ocean waters, the sea floor, and the atmosphere above the ocean.

PMEL *Pacific Marine Environmental Laboratory.* Monitors and predicts the physical and biological effects of man's activities on Pacific Coast estuarine, coastal, deep-ocean, and near-shore marine environments.

GLERL *Great Lakes Environmental Research Laboratory.* Studies hydrology, waves, currents, lake levels, biological and chemical processes, and lake-air interaction in the Great Lakes and their watersheds; forecasts lake ice conditions.

GFDL *Geophysical Fluid Dynamics Laboratory.* Studies the dynamics of geophysical fluid systems (the atmosphere, the hydrosphere, and the cryosphere) through theoretical analysis and numerical simulation using powerful, high-speed digital computers.

APCL *Atmospheric Physics and Chemistry Laboratory.* Studies cloud and precipitation physics, chemical and particulate composition of the atmosphere, atmospheric electricity, and atmospheric heat transfer, with focus on developing methods of beneficial weather modification.

NSSL *National Severe Storms Laboratory.* Studies severe-storm circulation and dynamics, and develops techniques to detect and predict tornadoes, thunderstorms, and squall lines.

WPL *Wave Propagation Laboratory.* Studies the propagation of sound waves and electromagnetic waves at millimeter, infrared, and optical frequencies to develop new methods for remote measuring of the geophysical environment.

ARL *Air Resources Laboratories.* Studies the diffusion, transport, and dissipation of atmospheric pollutants; develops methods of predicting and controlling atmospheric pollution; monitors the global physical environment to detect climatic change.

AL *Aeronomy Laboratory.* Studies the physical and chemical processes of the stratosphere, ionosphere, and exosphere of the Earth and other planets, and their effect on high-altitude meteorological phenomena.

SEL *Space Environment Laboratory.* Studies solar-terrestrial physics (interplanetary, magnetospheric, and ionospheric); develops techniques for forecasting solar disturbances; provides real-time monitoring and forecasting of the space environment.

U.S. DEPARTMENT OF COMMERCE
National Oceanic and Atmospheric Administration
BOULDER, COLORADO 80302